

---

# EXPLICITISING THE IMPLICIT INTERPRETABILITY OF DEEP NEURAL NETWORKS VIA DUALITY

---

A PREPRINT

**Chandrashekar Lakshminarayanan**  
 Indian Institute of Technology Madras  
 chandrashekar@cse.iitm.ac.in

**Amit Vikram Singh**  
 amitkvikram@gmail.com

**Arun Rajkumar**  
 Indian Institute of Technology Madras  
 arunr@cse.iitm.ac.in

March 31, 2022

## ABSTRACT

Recent work by Lakshminarayanan and Singh [2020] provided a dual view for fully connected deep neural networks (DNNs) with rectified linear units (ReLU). It was shown that (i) the information in the gates is analytically characterised by a kernel called the neural path kernel (NPK) and (ii) most critical information is learnt in the gates, in that, given the learnt gates, the weights can be retrained from scratch without significant loss in performance. Using the dual view, in this paper, we rethink the conventional interpretations of DNNs thereby explicitising the implicit interpretability of DNNs. Towards this, we first show new theoretical properties namely rotational invariance and ensemble structure of the NPK in the presence of convolutional layers and skip connections respectively. Our theory leads to two surprising empirical results that challenge conventional wisdom: (i) the weights can be trained even with a constant  $\mathbf{1}$  input, (ii) the gating masks can be shuffled, without any significant loss in performance. These results motivate a novel class of networks which we call deep linearly gated networks (DLGNs). DLGNs using the phenomenon of *dual lifting* pave way to more direct and simpler interpretation of DNNs as opposed to conventional interpretations. We show via extensive experiments on CIFAR-10 and CIFAR-100 that these DLGNs lead to much better interpretability-accuracy tradeoff.

## 1 Introduction

Despite their success deep neural networks (DNNs) are still largely considered as black boxes. The main issue is that in each layer of a DNN, the linear computation, i.e., multiplication by the weight matrix and the non-linear activations are entangled. The conventional interpretation is that such entanglement is the key to success of DNNs, in that, it allows DNNs to learn sophisticated structures in a layer-by-layer manner. In this work, we rethink this conventional interpretation using the recently developed dual view of DNNs Lakshminarayanan and Singh [2020].

Duality for DNNs with rectified linear units (ReLUs) attempts to understand DNNs via paths going from input to output instead of the conventional layer-by-layer view. Thanks to the gating property (i.e., ‘on/off’ states) of the ReLUs, the output can be expressed as a summation of contribution of the paths. The information in the gates is encoded in the so called *neural path feature* vector and the information in the weights are encoded in the *neural path value* vector, both of which are vectors in the dimension of the total number of paths. It follows then that the output is the inner product of the neural path feature and neural path value - this separates the gates from the weights analytically.

To understand the role of the gates, a deep gated network (DGN) (see Figure 2) was used to separate the gates from the weights. Using the DGN (as an experimental setup), two important insights were provided: (i) learning in the gates is the most crucial, in that, by using learnt gates in the gating network (by pre-training it), and retraining the

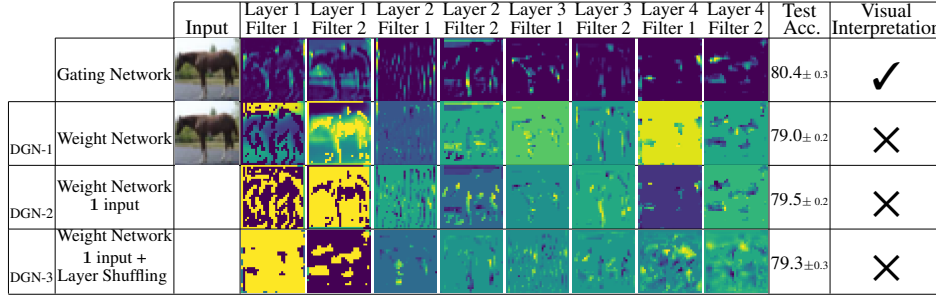


Figure 1: Shows the hidden layer outputs of 3 different convolutional DGNs namely DGN-1/2/3 (each with 4 hidden layers and 128 filters per layer). Each row has the input image to the network followed by the output of first 2 filters in each of the 4 hidden layers. All 3 DGNs have the same gating network which is shown in the top row. The 3 DGNs differ in the weight network as follows: (i) in DGN-1 in the second row, the weight network is provided with the input image and the layers are not shuffled, (ii) in DGN-2 in the third row, the weight network is provided with 1 as input and the layers are not shuffled, and (iii) in DGN-3 in the final row, the weight network is provided with 1 as input and the layers are shuffled. In the last two rows, the entry in the input image column ‘appears’ blank because it is the image of the 1 input to the weight network.

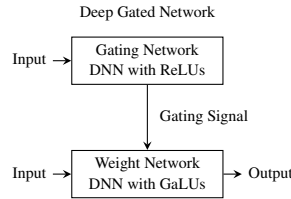


Figure 2: Deep Gated Network

weight network from scratch, the DGN can match the performance of the DNN, and (ii) in the limit of infinite width, learning the weights with fixed gates is equal to a kernel method with the neural path kernel (NPK)<sup>1</sup> which is the kernel associated with the neural path features.

While Lakshminarayanan and Singh [2020] provide an analytical expression for the NPK, the structural properties of the NPK were not entirely explored in their work. As we will see later, understanding these structural properties perhaps surprisingly leads to a fundamental rethinking of the conventional interpretation of DNNs. We establish this in this paper via novel theoretical and empirical contributions as listed below.

	DNN (Standard)	DGN ([Lakshminarayanan and Singh, 2020])	DLGN (this paper)
<b>Gating Network</b>	Not separate	Non-linear and hence	Linear and hence
<b>Weight Network</b>	Non-linearly entangled Non-interpretatable	Non-linear but unnecessary for interpretability (this paper)	interpretable (this paper)

Table 1: Upshot of the contributions in this paper

**Theoretical Contributions:** We present (Section 3) an unnoticed insight in prior work on fully connected networks that the NPK is a *product kernel* and is invariant to layer permutations. We present new results to show that (i) the NPK is *rotationally invariant* for convolutional networks with global average pooling, and (ii) the NPK is an *ensemble of many kernels* in the presence of skip connections.

**Key Empirical Contributions:** These theoretical results inspire the following empirical questions which lead to conventionally unexpected results.

*Constant Input:* We show that providing a constant 1 as input to the weight network of the DGN does not degrade performance. In the absence of ‘useful’ input, the conventional view that starting from the input, sophisticated features are learnt in a layer-by-layer manner fails to explain why the network still learns only with a constant 1 as input.

The invariance structure of the NPK allows us to explicitly break the layer-by-layer structure as follows.

<sup>1</sup>Lakshminarayanan and Singh [2020] showed that in a DGN the NPK is equal to a constant times the *neural tangent kernel* (NTK). The fact that infinite width DNNs are equivalent to the NTK was shown in [Jacot et al., 2018, Arora et al., 2019, Cao and Gu, 2019].

*Layer Shuffling:* We show that providing constant input together with permuting the layers (and then applying them as external masks) still does not degrade performance. We infer from our results that looking for ‘visually’ interpretable representations in the hidden layer outputs of the weights network is not meaningful and is not even an inherent property of the learnt weight network (see Figure 1).

**Modeling Contribution:** The insights we derive from the above surprising experiments are summarized in Table 1. In short, we conclude that DGNs not only provide a way to separate the weights from the gates, but more importantly also tell us that one must *not* look for *interpretability* in the weight network.

*Deep Linearly Gated Networks (DLGN):* Once we argue that the weight network has no interpretability value, we turn to the gating network. A standard DGN’s gating network has non-linear activations. We hypothesize that this is not essential. Towards this, we propose a novel architecture called Deep Linearly Gated Network which entirely eliminates the ReLUs (non-linearity) from the gating network thus making it a deep linear network. Our experiments (on CIFAR-10 and CIFAR-100) show that the DLGNs have much better interpretability-accuracy tradeoff than what a conventional route would suggest. We attribute and explain this using a phenomenon called *dual lifting* in DGN/DLGNs.

Our results show that the only useful source of interpretability in deep networks is in the linear gating network. This rethinking allows us to argue for the case that the deep learning community’s attempts at developing inbuilt algorithmic interpretability models must be via deep linear gating networks (DLGN).

**Related Works.** We now discuss prior works related most to our work and defer a more elaborate discussion to the appendix.

**Kernels:** Several works have examined theoretically as well as empirically two important kernels associated with a DNN namely its NTK based on the correlation of the gradients and the conjugate kernel based on the correlation of the outputs [Fan and Wang, 2020, Geifman et al., 2020, Liu et al., 2020, Chen et al., 2020, Xiao et al., 2020, Jacot et al., 2018, Arora et al., 2019, Novak et al., 2018, Lee et al., 2018, 2020]. In contrast, the NPK is based on the correlation of the gates. We do not build pure-kernel method with NPK, but use it as an aid to rethinking the conventional ‘hidden layer’ interpretation of finite width DNNs.

**Capacity:** Our experiments on destruction of layers, and providing constant  $\mathbf{1}$  input are direct consequences of the insights from dual view theory. These are not explained by mere capacity based studies showing DNNs are powerful to fit even random labelling of datasets [Zhang et al., 2016]. **Interpretability:** Rudin [2019] provides several compelling arguments for why it is important to build models that are interpretable by design as opposed to seeking *post-hoc* explanations for decisions of non-interpretable models. Rudin et al. [2021] discusses the grand challenges in interpretability. The DLGN in our paper resonates with the following aspect discussed in Rudin [2019], Rudin et al. [2021], i.e., most times the simpler models that are used to explain the decision of the more complicated non-interpretable models do not mimic the computations, thereby the explanations are not faithful which is an issue. The DLGN in our paper does not suffer from this issue because, the DLGN is obtained by rearranging the computations of a DNN with ReLUs in a mathematically principled manner.

## 2 Neural Path Kernel and Dual View

In this section, we first describe the recently developed dual path view of DNNs with ReLUs [Lakshminarayanan and Singh, 2020]. Among other things, the dual view leads to an understanding of (infinite width) DNNs as kernel methods with a novel kernel called the Neural Path Kernel (NPK). The NPK is related to the popular Neural Tangent Kernel (NTK). For a pair of input examples  $x, x'$  and network weights  $\Theta \in \mathbb{R}^{d_{\text{net}}}$ , the NTK is defined as follows:

$$\text{NTK}(x, x') = \langle \nabla_{\Theta} \hat{y}(x), \nabla_{\Theta} \hat{y}(x') \rangle, \quad \text{where}$$

$\hat{y}_{\Theta}(\cdot) \in \mathbb{R}$  is the DNN output. Prior works [Jacot et al., 2018, Arora et al., 2019, Cao and Gu, 2019] have shown that, as the width of the DNN goes to infinity, the NTK matrix converges to a limiting deterministic matrix  $\text{NTK}_{\infty}$ , and training an infinitely wide DNN is equivalent to a kernel method with  $\text{NTK}_{\infty}$ .

The dual view gives a more fine grained understanding of a fully connected DNN with ‘ $d$ ’ layers and ‘ $w$ ’ hidden units in each layer. Specifically, in the dual view, the computations are broken down path-by-path. The input and the gates (in each path) are encoded in a *neural path feature vector* -  $\phi_{\Theta}(x) \in \mathbb{R}^P$  and the weights (in each path) are encoded in a *neural path value vector* -  $v_{\Theta}(x) \in \mathbb{R}^P$ , where  $P$  is the total number of paths. The output of the DNN was shown to be the inner product of these two vectors:

$$\hat{y}_{\Theta}(x) = \langle \phi_{\Theta}(x), v_{\Theta} \rangle = \sum_{p=1}^P \phi_{\Theta}(x, p) v_{\Theta}(p) \quad (1)$$

Furthermore, using the dual view, a novel kernel called NPK was defined as follows:

$$\text{NPK}_{\Theta}(x, x') \triangleq \langle \phi_{\Theta}(x), \phi_{\Theta}(x') \rangle = \langle x, x' \rangle \mathbf{overlap}_{\Theta}(x, x')$$

where  $\mathbf{overlap}_{\Theta}(x, x')$  is equal to the total number of paths that get activated for both inputs  $x$  and  $x'$ .

The dual view led Lakshminarayanan and Singh [2020] to the question of seeking the *real source of learning* in DNNs. To understand this, they propose the **Deep Gated Network (DGN)** which is a setup to separate the gates from the weights. Consider a DNN with ReLUs with weights  $\Theta \in \mathbb{R}^{d_{\text{net}}}$ . The DGN *corresponding* to this DNN (Figure 2) has two networks of *identical architecture* (to the DNN) namely the gating network and the weight network with distinct weights  $\Theta^g \in \mathbb{R}^{d_{\text{net}}}$  and  $\Theta^v \in \mathbb{R}^{d_{\text{net}}}$ . The gating network has ReLUs which turn ‘on/off’ based on their pre-activation signals, and the weight network has gated linear units (GaLUs) [Fiat et al., 2019, Lakshminarayanan and Singh, 2020], which multiply their respective pre-activation inputs by the external gating signals provided by the gating network. Since both the networks have identical architecture, the ReLUs and GaLUs in the respective networks have a one-to-one correspondence. Gating network realises  $\phi_{\Theta^g}(x)$  by turning ‘on/off’ the corresponding GaLUs in the weight network. The weight network realises  $v_{\Theta^v}$  and computes the output  $\hat{y}_{\text{DGN}}(x) = \langle \phi_{\Theta^g}(x), v_{\Theta^v} \rangle$ .

The main result of Lakshminarayanan and Singh [2020] shows that under mild conditions, for a fully connected DGN, the NTK and NPK are related by a constant factor. Specifically, in the limit of infinite width, assuming all the weights are initialized from the set  $\{\sigma, -\sigma\}$  with equal probability, they show the following:

$$\text{NTK}(x, x') \rightarrow d \cdot \sigma^{2(d-1)} \cdot \text{NPK}(x, x'), \quad \text{as } w \rightarrow \infty$$

Using extensive experiments in the DGN setup that separates the gates from the weights, Lakshminarayanan and Singh [2020] were able to demonstrate that the real source of learning is in the gates and that learning the gates is key for good performance.

### 3 Theoretical Results

In this section, we give novel theoretical results concerning the Neural Path Kernel. These results will help us understand DGNs better and will lead us to devise novel experiments with conventionally unexpected results. Our first result is based on a simple but very significant observation about the structure of the Neural Path Kernel. Recall that the NPK depends on  $\mathbf{overlap}(x, x')$ . We show that this term can in fact be written in a product form and so the NPK kernel is in fact a product kernel.

**Theorem 3.1. (NPK is a Product Kernel)** Let  $G_l(x) \in [0, 1]^w$  denote the gates in layer  $l \in \{1, \dots, d-1\}$  for input  $x \in \mathbb{R}^{d_{\text{in}}}$ . Then

$$\mathbf{overlap}(x, x') = \prod_{l=1}^{(d-1)} \langle G_l(x), G_l(x') \rangle$$

Thus the NPK for a fully connected DGN is given by

$$\text{NPK}(x, x') = \langle x, x' \rangle \cdot \prod_{l=1}^{(d-1)} \langle G_l(x), G_l(x') \rangle$$

Theorem 3.1 provides the most simplest kernel expression that characterises the information in the gates. The product structure, as we will see later, is key to devise experiments that break the layer by layer structure of DGNs.

While only fully connected DGNs were analyzed in Lakshminarayanan and Singh [2020], we go further and derive the structure of NPK for two important architectures - ConvNets with global-average-pooling and ResNet with skip connections. The next two theorems make this precise. In what follows, let the circular rotation of vector  $x \in \mathbb{R}^{d_{\text{in}}}$  by ‘ $r$ ’ co-ordinates be defined as  $\text{rot}(x, r)(i) = x(i+r)$ , if  $i+r \leq d_{\text{in}}$  and  $\text{rot}(x, r)(i) = x(i+r-d_{\text{in}})$  if  $i+r > d_{\text{in}}$ .

**Theorem 3.2. (NPK for ConvNets is rotationally invariant)** The Neural Path Kernel for a Convolutional Neural Network is given as follows:

$$\text{NPK}^{\text{CONV}}(x, x') = \sum_{r=0}^{d_{\text{in}}-1} \langle x, \Lambda \text{rot}(x', r) \rangle$$

where  $\Lambda = \mathbf{overlap}(\cdot, x, \text{rot}(x', r))$ .

Here  $\Lambda$  is a diagonal matrix whose diagonal entries correspond to the total number of common paths starting from input node  $i$  active for both inputs  $x$  and  $x'$ . Note that in the fully connected case,  $\mathbf{overlap}(i, x, x')$  is identical for all  $i = 1, \dots, d_{\text{in}}$ , and hence  $\langle x, \Lambda x' \rangle$  becomes  $\langle x, x' \rangle \cdot \mathbf{overlap}(x, x')$ . This in general will not be the case for ConvNets.

Architecture	Dataset	WITHOUT SHUFFLING			WITH SHUFFLING	
		DNN	DGN	DGN-ALLONES	DGN	DGN-ALLONES
FC4	MNIST	98.5±0.1	98.6±0.1	98.6±0.1	98.6±0.1	98.6±0.1
CONV4	CIFAR-10	80.4±0.3	79.0±0.2	79.0±0.2	79.5±0.2	79.3±0.3
VGG	CIFAR-10	93.6±0.2	93.5±0.1	93.4±0.1	93.5±0.1	93.5±0.1
ResNet	CIFAR-10	94.0±0.2	93.8±0.1	93.9±0.1	93.5±0.3	93.5±0.1

**Models.** FC4: Fully connected network with 4 hidden layers, and 128 units per layer. CONV4: Convolutional network with 4 hidden layers, and 128 filters per layer, followed by global-average-pooling, and output layer. VGG is VGG-16 and ResNet is ResNet-110 from Mikler [2019]. **Shuffling.** The last two columns contains the results after shuffling. Please look at Figure 3 to see how to shuffle the layers in FC4 (DGN) and CONV4 (DGN). Please look at Appendix A to see how to shuffle VGG and ResNet.

Table 2: Entries in the first 3 columns and the  $3^{rd}$  row for VGG are averaged over 5 independent runs. The entries in the last row for ResNet are averaged over 3 independent runs. The entries in the first two rows and last two columns are averaged over the 23 models obtained via permuting the layers (here each model is run once). The results in this table are in the setting wherein the gating network of the DGNs are pre-trained. However, the same results also hold even when the gating network is trained from scratch simultaneously alongside the weight network, and this is shown in Table 3. In short, pre-training the gating network is not critical for the surprising results in the constant input and layer shuffling scenarios.

The right hand side of the expression for  $NPK^{CONV}$  can further be written as  $\sum_{r=0}^{d_{in}-1} \sum_{i=1}^{d_{in}} x(i)rot(x', r)(i) \mathbf{overlap}(i, x, rot(x', r))$ , where the inner ‘ $\Sigma$ ’ is the inner product between  $x$  and  $rot(x', r)$  weighted by **overlap** and the outer ‘ $\Sigma$ ’ covers all possible rotations, which in addition to the fact that all the variables internal to the network rotate as the input rotates, results in the rotational invariance. That said, rotational invariance is not a new observation; it was shown by Li et al. [2019] the NTK for ConvNets with global-average-pooling are rotationally invariant. Importance of Theorem 3.2 lies in the fact that it gives a fine grained expression for the kernel by explicitising the gates, a fact which will be used critically in the experiments.

We next consider a ResNet with ‘ $(b + 2)$ ’ blocks and ‘ $b$ ’ skip connections between the blocks. Each block is a fully connected (FC) network of depth ‘ $d_{blk}$ ’ and width ‘ $w$ ’. There are  $2^b$  many sub-FCNs within this ResNet. Note that the blocks being fully connected is for expository purposes, and the result continue to hold for any kind of block.

Let  $2^{[b]}$  denote the power set of  $[b]$  and let  $\mathcal{J} \in 2^{[b]}$  denote any subset of  $[b]$ . Define the ‘ $\mathcal{J}^{th}$ ’ sub-FCN of the ResNet to be the fully connected network obtained by (i) including block $_j, \forall j \in \mathcal{J}$  and (ii) ignoring block $_j, \forall j \notin \mathcal{J}$ . In Theorem 3.3 below,  $NPK_{\mathcal{J}}^{FC}$  is the NPK of the  $\mathcal{J}^{th}$  FCN.

**Theorem 3.3. (NPK for ResNet is an Ensemble)** The NPK structure for Res-Net is given by

$$NPK^{RES} = \sum_{\mathcal{J} \in 2^{[b]}} NPK_{\mathcal{J}}^{FC},$$

To the best of our knowledge, this is the first theoretical result to show that ResNets have an ensemble structure, where each kernel in the ensemble, i.e.,  $NPK_{\mathcal{J}}^{FC}$  corresponds to one of the  $2^b$  sub-architectures. We will see in the next section how the ensemble property leads to surprising empirical consequences.

**Remark:** We also derive that in limit of infinite width, the NTKs,  $NTK^{CONV}$  and  $NTK^{RES}$  is equal to a constant times  $NPK^{CONV}$  and  $NPK^{RES}$ . We defer the formal results to the appendix as these are not the main focus of this paper.

## 4 Weight Network is Unnecessary for Interpretability

The theoretical understanding of the Neural Path Kernel in the previous section leads us to the following fundamental claim about Deep Gated Networks namely *the weight network is unnecessary for interpretability*. We perform two sets of experiments to back this claim. These experimental conclusions would apriori seem counter intuitive and challenge the conventional understanding of what a network is learning. However, viewed with the insight gained from the theoretical results based on the dual view, these conclusions make sense and will lead us to propose a more interpretable architecture in the next section.

### 4.1 Constant Input Does Not Hurt Performance

Our first experiment attacks the input to a standard DGN. A standard DGN uses the same input to both the gating network and weight network. In our modified set up, we only supply the input to the gating network and a constant all ones vector as input to the weight network. We refer to the resulting network architecture as DGN-ALLONES. From a conventional wisdom of ‘layer by layer’ learning of sophisticated features, one would expect a significant drop in the performance when the input is made constant. However, we show in Table 2, this is not the case.

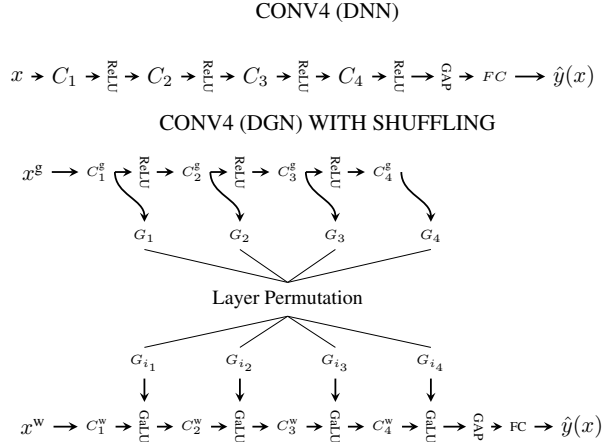


Figure 3: Top: CONV4 (DNN). Bottom: CONV4 (DGN) along with mechanism to shuffle the gating masks. Here  $x^g$  and  $x^w$  denote the input to the gating and weight network respectively. Here the gates  $G_1, G_2, G_3, G_4$  are generated by the gating network and are permuted as  $G_{i_1}, G_{i_2}, G_{i_3}, G_{i_4}$  before applying to the weight network. Shuffling of FC4 (DGN) is similar to CONV4 (DGN). There are 24 possible permutations of the gating masks. For FC4 and CONV4, the results of the models with identity permutation of layers are in column WITHOUT SHUFFLING in Table 2 and the results of the 23 other models are in the column WITH SHUFFLING in Table 2.

**Theoretical Justification:** We will now explain how the results in Table 2 follows from results in the previous section. In the fully connected case, the expression on right hand side of the NPK expression in Theorem 3.1 becomes  $\prod_{l=1}^{d-1} \langle G_l(x), G_l(x') \rangle$ , i.e., the kernel still has information about the input encoded via the gates. In the case of convolutional networks, the expression in Theorem 3.2 becomes  $\sum_{r=0}^{d_{in}-1} \sum_{i=1}^{d_{in}} \mathbf{overlap}(i, x, rot(x', r))$ . The key novel insight is that the rotational invariance is not lost and **overlap** matrix measures the correlation of the paths which in turn depends on the correlation of the gates. In the case of ResNets, as the  $\text{NPK}^{\text{RES}}$  of the residual networks is an ensemble, the property of the block level kernel (i.e., of  $\text{NPK}^{\text{FC}}/\text{NPK}^{\text{CONV}}$ ) translates to  $\text{NPK}^{\text{RES}}$ .

### 4.2 Layer Shuffling Does not Hurt Performance

Our second experiment attacks the hidden layers of the weight network of standard DGN. In addition to the all ones input, we now also randomly shuffle the hidden layers i.e., the gating masks are applied post layer shuffling (See Figure 3). Again, if the conventional wisdom about layer-by-layer learning were true, then the performance after layer shuffling must take a big hit. We show in Table 2 that this is not the case.

**Theoretical Justification:** Recall that in the NPK expression for the fully connected case in Theorem 3.1,  $\prod_{l=1}^{d-1} \langle G_l(x), G_l(x') \rangle$  is permutation invariant, and hence permuting the layers has no effect, in that, it leaves the NPK expression unchanged. Similarly, permuting the layers does not destroy the rotational invariance in Theorem 3.2. This is because, due to circular convolutions all the internal variables of the network rotate as the input rotates. Permuting the layers only affects the ordering of the layers, and does not affect the fact that the gates rotate if the input rotates. As explained previously, ResNet being an ensemble of block level kernels, inherits the permutation invariance property from the blocks (be it fully connected or convolutional).

**Remark:** In the case of ResNets, even removing layers does not hurt performance. The ensemble behaviour of ResNet and presence of  $2^b$  architectures was observed by Veit et al. [2016], however without any concrete theoretical formalism. Veit et al. [2016] showed empirically that removing single layers from ResNets at test time does not noticeably affect their performance, and yet removing a layer from architecture such as VGG leads to a dramatic loss in performance. Theorem 3.3 can be seen to provide a theoretical justification for this empirical result. The ResNet

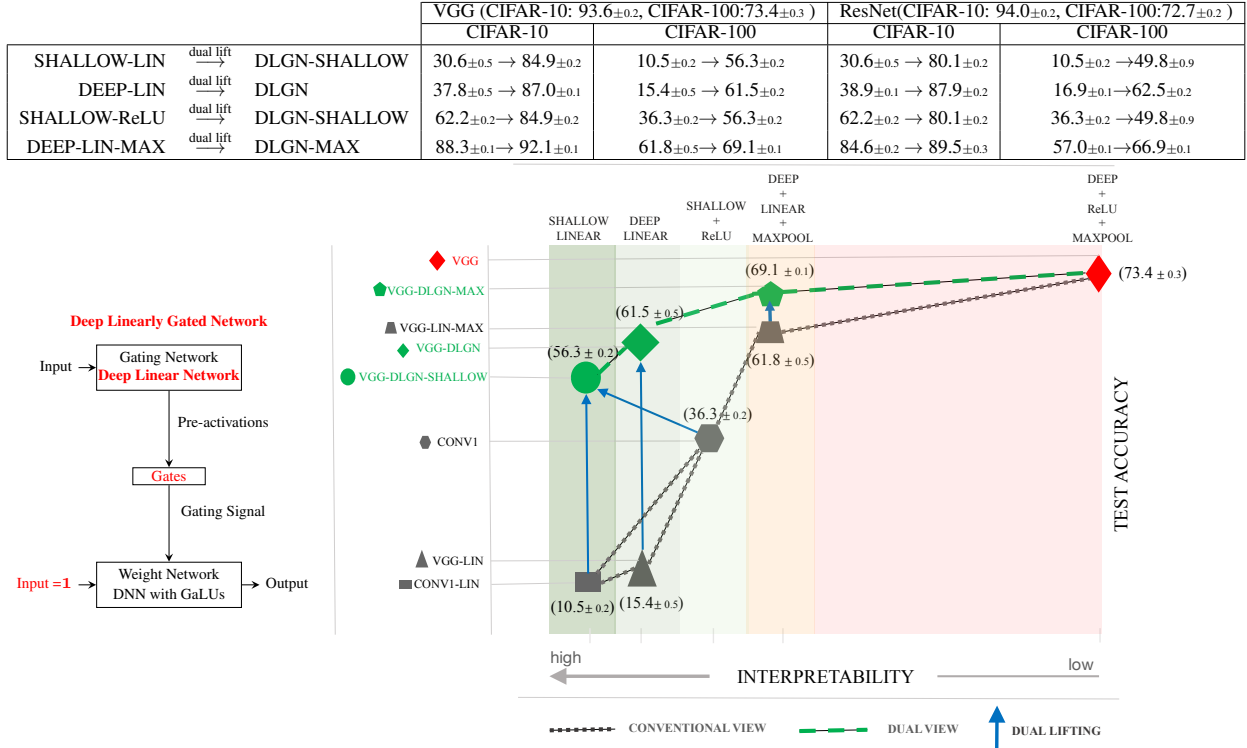


Figure 4: **Left:** Shows the DLGN which is DGN whose gating network is linear. In the DLGN, both the gating and weight networks are trained simultaneously using the same protocol (step size, learning rate, optimiser) followed to train the corresponding DNNs. **Right:** Shows the interpretability-accuracy tradeoff plot for the various models considered. The gray path shows models that are obtained via the conventional view, and the green path shows models obtained via DLGN (proposed in this paper) by dual lifting (see Section 4.3). **Top:** Shows the tabular column of test accuracies of all the models. Here, the results for ResNet variants are averaged over 3 independent runs and the results for other models are averaged over 5 independent runs.

inherits the invariances of the block level kernel. In addition, the ensemble structure allows to even remove layers. In other words, due to the ensemble structure a ResNet is robust to failures, in particular, the insight is that even if one or many of the kernels in the ensemble are corrupt, the good ones can compensate.

**Remark:** A qualitative justification of the above results can be found in Figure 1 (see caption for details).

### 4.3 Dual Lifting

The above experiments lead to the important conclusion that the non-linear weight network of DGNs while crucial for ensuring good performance, must not be used to interpret what is being learnt in the layers. Then, a natural question is to understand the role of the weight network. This is easy to answer from the dual viewpoint, paying attention to the phenomena of what we call as *dual lifting*, which we explain below.

The gating network provides the pre-activations to the GaLUs in the weight network. By switching on/off the GaLUs, the paths in the weight network are turned on/off. This causes the **dual lifting** of the features in the form of layer outputs from the gating network to get **lifted** to a neural path feature vector, i.e., a vector in the dimension of the total number of paths. Now, the neural path value is a function of the weights in the weight network and finally the *dual linearity* i.e., the inner product between the neural path feature and neural path value is computed. In short, dual lifting causes the information in the layers of the gating network to be thrown into the dimension of paths.

### 4.4 Implications

As a natural consequence of the fact that the weight network is not needed for interpretation, any attempt at interpreting DGNs must focus on what is being learnt in the gating network. However, DGNs have non-linearity (ReLU) in the

gating network which make interpretations harder. A natural question is then *Is the ReLU in the Gating Network crucial for good performance?*. Surprisingly, the answer seems to be a no. We discuss this in the next section in detail.

## 5 Rethinking Interpretability via Deep Linearly Gated Networks

The experimental results of the previous section rule out the necessity for looking at the weight network of the DGN for interpretability. Thus we turn our attention to the gating network. To make DGNs interpretable, we propose the Deep Linearly Gated Network (DLGN) (see left hand side of Figure 4) wherein we completely eliminate the non-linearity of the gating network by removing the ReLU activations. Before we explain the results that we obtain for DLGNs, we take a step back and discuss interpretability in general. This will help us contextualise our results better.

The simplest *interpretable* model is the shallow linear model. In this model, while retaining linearity, one can increase it’s complexity by introducing deep layers. Instead of adding deep layers, if one adds ReLU to a shallow linear model, one gets the well studied ReLU networks with single hidden layer Chizat and Bach [2018], Zhang et al. [2019], Li and Liang [2018], Zhong et al. [2017], Li and Yuan [2017], Ge et al. [2017], Du et al. [2018]. However, the non-linearity in the ReLU makes it less interpretable compared to a deep linear model. As a next step, one might want to add the standard deep learning *tricks* such as striding, average/max-pooling and batch normalisation to a deep linear model. Out of these tricks, only max-pooling is non-linear. Yet, interpretability wise it may be considered a benign form of non-linearity in comparison to ReLU, the reason being that, max-pooling acts directly on the input as opposed to ReLU which acts on the input transformed by a weight vector. As max-pooling is essentially a sub-sampling operation a deep linear model with max-pooling could potentially be interpreted by understanding the linear part and max-pooling separately. Once non-linearity is introduced in the form of say ReLU in deep networks, one typically loses interpretability. Thus one can arrange the increasing levels of interpretable models as follows:

$$\begin{aligned}
 &\text{Shallow Linear} > \text{Deep Linear} > \\
 &\text{Shallow} + \text{ReLU} > \text{Deep Linear} + \text{MaxPool} > \\
 &\text{Deep} + \text{ReLU} > \text{Deep} + \text{MaxPool} + \text{ReLU}
 \end{aligned}
 \tag{2}$$

The conventional viewpoint is that as we gain interpretability, we lose accuracy in proportional measure. In practice then one resorts to choosing accuracy over interpretability and then attempts to interpret/explain the model in a post-hoc fashion Ribeiro et al. [2016], Selvaraju et al. [2017], Chattopadhyay et al. [2018]. However, several recent works have pointed out the need for developing built-in interpretable models i.e., making deep models more interpretable and avoiding taking a post-hoc view of the same Rudin [2019], Rudin et al. [2021]. We argue that this is possible by showcasing such a model. In fact, one can still have *essentially linear* interpretable models which perform almost as well as DNNs/DGNs thanks to the phenomenon of *Dual Lifting* in weight network. The main idea is that we start with a standard DGN and make two key changes: (i) we make the gating network linear and (ii) we give all ones (non-useful) input to the weight network. We refer to this model a Deep Linearly Gated Network. The network still has GaLU activations as in DGNs but only in the weight network which we already know from Section 4 does not play a role in interpretability. Thus, non-linearity is present to perform a *lifting* from the primal space to the dual space. By clearly separating the linear part from the non-linear part and noting that the non-linear part does not play a role in interpretability, we gain the advantages of both worlds.

We describe our results in Figure 4 (the table in the top and the plot in the bottom right). The figure lays out the landscape of interpretable models starting from the shallow linear model all the way upto the standard Deep + Maxpool + ReLU models. We first describe the models considered in detail below.

**Models Considered:** Our aim is to create one conventional model for each of the cases in the inequality in Equation (2) and the corresponding DLGN counterpart. CONV1 has 1 convolutional layer with 512 filters, followed by ReLU, global-average-pooling and output layer (this is the shallow + ReLU model). CONV1-LIN is same as CONV1 with the ReLU activations replaced by identity activation (this is the shallow linear model). VGG-LIN is same as VGG with average pooling instead of max-pooling (to ensure linearity) and ReLUs replaced by identity activation. VGG-LIN-MAX is VGG (i.e., with max-pooling) and ReLUs replaced by identity activation. VGG-DLGN is the DLGN counterpart of VGG (the architecture is in Figure 7 in the appendix). VGG-DLGN-SHALLOW is obtained by modifying the gating network of VGG-DLGN as follows: the pre-activations to the gates are generated by  $d$  shallow linear convolutional networks (the architecture is in Figure 8 in the appendix). VGG-DLGN-MAX is same as VGG-DLGN, however with max-pooling instead of average pooling.

Conventional thinking to understand interpretability-accuracy tradeoff would suggest increasing model complexity one step at a time starting right from shallow linear networks i.e., moving along one of the gray paths in Figure 4. The proposed model, DLGN and it’s corresponding variants for each of the cases, by exploiting *Dual Lifting*, outperforms the conventional models at every stage. This corresponds to the green path in Figure 4. By taking the green path, one



retains as much interpretability as their counterpart models in the conventional way of thinking while still gaining accuracy. This is the primary advantage of DLGNs.

**Lifting:** It is interesting to note that there is a significant gain due to lifting from the Shallow Linear Model to the DLGN-Shallow model. The gain decreases as one adds deep layers followed by MaxPool. This is expected as the effect of the non-linear, non-interpretable weights network is most pronounced when the original model that it is compared against is linear (and shallow). As one introduces some form of non-linearity (MaxPool or ReLU), the lifting helps lesser.

**Deep Linear + MaxPool:** We observe that adding max-pool to deep linear models results in significant boost in performance (VGG/ResNet-LIN-MAX performs better than VGG/ResNet-LIN). It is worth noting that dual lifting of VGG-LIN-MAX to VGG-DLGN-MAX further boosts the performance achieving accuracies of **69.1%** and **92.1%** on CIFAR-10 and CIFAR-100 respectively, which are within **4.3%** and **1.5%** of the performance of VGG on the respective datasets. As discussed before, VGG-DLGN-MAX is worthy of further interpretation by separately understanding the linear part and max-pooling. Also, it would be an interesting future study to understand the reason for the boost in performance when max-pooling is added to a deep linear model.

**Deep Linear and Shallow Linear:** While the representation power of the deep and shallow linear networks is the same, the difference between them is that of optimisation. We observe that both these models perform poorly in both CIFAR-10 as well as CIFAR-100. Since our main focus has been in interpretable models that also achieve reasonable test accuracy, we did not probe further into these two models. Nevertheless, deep linear networks have been studied well in the literature, especially in connection to the optimisation of deep networks Shamir [2019], Du and Hu [2019], Saxe et al. [2013], Ji and Telgarsky [2018].

**SHALLOW-ReLU vs DLGN-SHALLOW:** Note that the gating network of the DLGN-SHALLOW comprises of several shallow linear networks in parallel, each which in turn trigger the gates of a layer in the corresponding weight network. Thus if one dual lifts a SHALLOW-ReLU model we obtain a DLGN-SHALLOW model (as seen in Figure 4). We observe that VGG-DLGN-SHALLOW performs better than CONV1. Note that VGG-DLGN-SHALLOW is better than CONV1 both in terms of interpretability and accuracy.

**Dual Lifting and Standard DNNs:** Given the performance gain due to dual lifting, a natural question to ask is whether dual lifting is a phenomena solely restricted to DGN/DLGNs or can it also be used to improve the performance of standard DNNs. This is answered by looking at standard DNNs with ReLUs to be models that have their gating and weight networks to be one and the same, and since dual lifting happens in the weight network, it follows that *dual lifting is implicit in standard DNNs with ReLUs*. Seen this way, one can attribute the success of standard DNNs with ReLUs also to dual lifting.

**Remark:** The trend for the ResNet variants also follows in a similar manner as VGG variants (see table on top of Figure 4). We also observe that the performance gap between the various models is less on CIFAR-10 and more pronounced in CIFAR-100, which is expected since CIFAR-100 (with 100 classes) is a harder dataset than CIFAR-10 (with 10 classes).

## 6 Conclusion

In this paper, we rethink the conventional interpretations of DNNs by taking a dual view. By exploiting novel theoretical properties of Neural Path Kernel that we identify, we demonstrate via extensive experiments that only the Gating network of a Deep Gated Network is necessary for interpretability. We propose Deep Linearly Gated Networks, an interpretable counterpart to DGNs and show how it makes use of the phenomenon of dual lifting to improve accuracy over conventional approaches while maintaining interpretability.

We believe our results on the surprisingly good performance of DLGNs (as compared to DGNs) would motivate DNN researchers to take a closer look at domain specific understanding of DLGNs. Future work includes understanding DLGNs from the point of view of adversarial attacks.

## References

- Chandrashekar Lakshminarayanan and Amit Vikram Singh. Neural path features and neural path kernel: Understanding the role of gates in deep learning. *Advances in Neural Information Processing Systems*, 33, 2020.
- Arthur Jacot, Franck Gabriel, and Clément Hongler. Neural tangent kernel: Convergence and generalization in neural networks. In *Advances in neural information processing systems*, pages 8571–8580, 2018.

- Sanjeev Arora, Simon S Du, Wei Hu, Zhiyuan Li, Russ R Salakhutdinov, and Ruosong Wang. On exact computation with an infinitely wide neural net. In *Advances in Neural Information Processing Systems*, pages 8139–8148, 2019.
- Yuan Cao and Quanquan Gu. Generalization bounds of stochastic gradient descent for wide and deep neural networks. In *Advances in Neural Information Processing Systems*, pages 10835–10845, 2019.
- Zhou Fan and Zhichao Wang. Spectra of the conjugate kernel and neural tangent kernel for linear-width neural networks. *arXiv preprint arXiv:2005.11879*, 2020.
- Amnon Geifman, Abhay Yadav, Yoni Kasten, Meirav Galun, David Jacobs, and Ronen Basri. On the similarity between the laplace and neural tangent kernels. *arXiv preprint arXiv:2007.01580*, 2020.
- Chaoyue Liu, Libin Zhu, and Mikhail Belkin. On the linearity of large non-linear models: when and why the tangent kernel is constant. *Advances in Neural Information Processing Systems*, 33, 2020.
- Zixiang Chen, Yuan Cao, Quanquan Gu, and Tong Zhang. A generalized neural tangent kernel analysis for two-layer neural networks. *Advances in Neural Information Processing Systems*, 33, 2020.
- Lechao Xiao, Jeffrey Pennington, and Samuel Schoenholz. Disentangling trainability and generalization in deep neural networks. In *International Conference on Machine Learning*, pages 10462–10472. PMLR, 2020.
- Roman Novak, Lechao Xiao, Yasaman Bahri, Jaehoon Lee, Greg Yang, Jiri Hron, Daniel A Abolafia, Jeffrey Pennington, and Jascha Sohl-dickstein. Bayesian deep convolutional networks with many channels are gaussian processes. In *International Conference on Learning Representations*, 2018.
- Jaehoon Lee, Yasaman Bahri, Roman Novak, Samuel S Schoenholz, Jeffrey Pennington, and Jascha Sohl-Dickstein. Deep neural networks as gaussian processes. In *International Conference on Learning Representations*, 2018.
- Jaehoon Lee, Samuel S Schoenholz, Jeffrey Pennington, Ben Adlam, Lechao Xiao, Roman Novak, and Jascha Sohl-Dickstein. Finite versus infinite neural networks: an empirical study. *arXiv preprint arXiv:2007.15801*, 2020.
- Chiyuan Zhang, Samy Bengio, Moritz Hardt, Benjamin Recht, and Oriol Vinyals. Understanding deep learning requires rethinking generalization. *arXiv preprint arXiv:1611.03530*, 2016.
- Cynthia Rudin. Stop explaining black box machine learning models for high stakes decisions and use interpretable models instead. *Nature Machine Intelligence*, 1(5):206–215, 2019.
- Cynthia Rudin, Chaofan Chen, Zhi Chen, Haiyang Huang, Lesia Semenova, and Chudi Zhong. Interpretable machine learning: Fundamental principles and 10 grand challenges. *arXiv preprint arXiv:2103.11251*, 2021.
- Jonathan Fiat, Eran Malach, and Shai Shalev-Shwartz. Decoupling gating from linearity. *CoRR*, abs/1906.05032, 2019. URL <http://arxiv.org/abs/1906.05032>.
- Zhiyuan Li, Ruosong Wang, Dingli Yu, Simon S Du, Wei Hu, Ruslan Salakhutdinov, and Sanjeev Arora. Enhanced convolutional neural tangent kernels. *arXiv preprint arXiv:1911.00809*, 2019.
- Szymon Mikler. Resnets in tensorflow2. <https://github.com/gahaalt/resnets-in-tensorflow2>, 2019.
- Andreas Veit, Michael Wilber, and Serge Belongie. Residual networks behave like ensembles of relatively shallow networks. *arXiv preprint arXiv:1605.06431*, 2016.
- Lenaic Chizat and Francis Bach. On the global convergence of gradient descent for over-parameterized models using optimal transport. *arXiv preprint arXiv:1805.09545*, 2018.
- Xiao Zhang, Yaodong Yu, Lingxiao Wang, and Quanquan Gu. Learning one-hidden-layer relu networks via gradient descent. In *The 22nd international conference on artificial intelligence and statistics*, pages 1524–1534. PMLR, 2019.
- Yuanzhi Li and Yingyu Liang. Learning overparameterized neural networks via stochastic gradient descent on structured data. *arXiv preprint arXiv:1808.01204*, 2018.
- Kai Zhong, Zhao Song, Prateek Jain, Peter L Bartlett, and Inderjit S Dhillon. Recovery guarantees for one-hidden-layer neural networks. In *International conference on machine learning*, pages 4140–4149. PMLR, 2017.
- Yuanzhi Li and Yang Yuan. Convergence analysis of two-layer neural networks with relu activation. *arXiv preprint arXiv:1705.09886*, 2017.
- Rong Ge, Jason D Lee, and Tengyu Ma. Learning one-hidden-layer neural networks with landscape design. *arXiv preprint arXiv:1711.00501*, 2017.
- Simon Du, Jason Lee, Yuandong Tian, Aarti Singh, and Barnabas Poczos. Gradient descent learns one-hidden-layer cnn: Don’t be afraid of spurious local minima. In *International Conference on Machine Learning*, pages 1339–1348. PMLR, 2018.

- Marco Tulio Ribeiro, Sameer Singh, and Carlos Guestrin. "why should i trust you?" explaining the predictions of any classifier. In *Proceedings of the 22nd ACM SIGKDD international conference on knowledge discovery and data mining*, pages 1135–1144, 2016.
- Ramprasaath R Selvaraju, Michael Cogswell, Abhishek Das, Ramakrishna Vedantam, Devi Parikh, and Dhruv Batra. Grad-cam: Visual explanations from deep networks via gradient-based localization. In *Proceedings of the IEEE international conference on computer vision*, pages 618–626, 2017.
- Aditya Chattopadhyay, Anirban Sarkar, Prantik Howlader, and Vineeth N Balasubramanian. Grad-cam++: Generalized gradient-based visual explanations for deep convolutional networks. In *2018 IEEE winter conference on applications of computer vision (WACV)*, pages 839–847. IEEE, 2018.
- Ohad Shamir. Exponential convergence time of gradient descent for one-dimensional deep linear neural networks. In *Conference on Learning Theory*, pages 2691–2713, 2019.
- Simon S Du and Wei Hu. Width provably matters in optimization for deep linear neural networks. *arXiv preprint arXiv:1901.08572*, 2019.
- Andrew M Saxe, James L McClelland, and Surya Ganguli. Exact solutions to the nonlinear dynamics of learning in deep linear neural networks. *arXiv preprint arXiv:1312.6120*, 2013.
- Ziwei Ji and Matus Telgarsky. Gradient descent aligns the layers of deep linear networks. *arXiv preprint arXiv:1810.02032*, 2018.
- Randall Balestriero et al. A spline theory of deep learning. In *International Conference on Machine Learning*, pages 374–383, 2018.
- Randall Balestriero and Richard G Baraniuk. From hard to soft: Understanding deep network nonlinearities via vector quantization and statistical inference. *arXiv preprint arXiv:1810.09274*, 2018.
- Rupesh Kumar Srivastava, Klaus Greff, and Jürgen Schmidhuber. Highway networks. *arXiv preprint arXiv:1505.00387*, 2015.
- Prajit Ramachandran, Barret Zoph, and Quoc V. Le. Searching for activation functions, 2018. URL <https://openreview.net/forum?id=SkBYyZRZ>.
- Joel Veness, Tor Lattimore, Avishkar Bhoopchand, David Budden, Christopher Mattern, Agnieszka Grabska-Barwinska, Peter Toth, Simon Schmitt, and Marcus Hutter. Gated linear networks. *arXiv preprint arXiv:1910.01526*, 2019.
- David G Clark, LF Abbott, and SueYeon Chung. Credit assignment through broadcasting a global error vector. *arXiv preprint arXiv:2106.04089*, 2021.
- Diederik P. Kingma and Jimmy Ba. Adam: A method for stochastic optimization, 2014.

## A Shuffling in VGG and ResNet

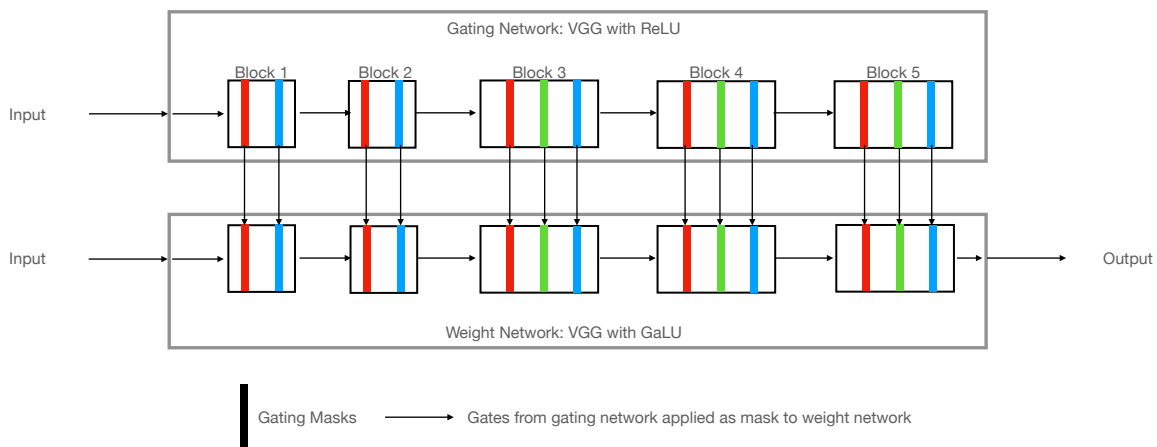


Figure 5: Shows VGG (DGN).

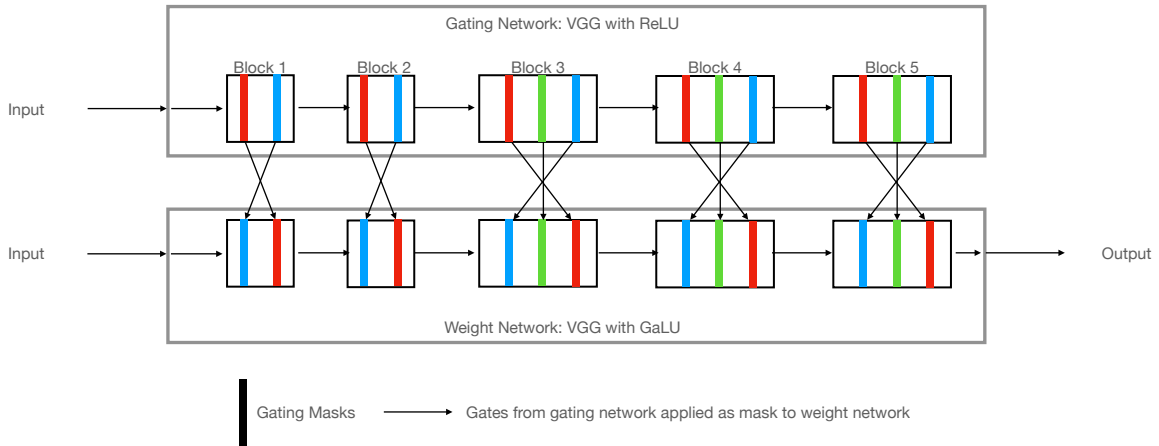


Figure 6: Shows shuffling of gating masks in VGG (DGN) in the last two columns,  $3^{rd}$  row in Table 2. The shuffling of ResNet (DGN) is similar. VGG contains 5 blocks each with filter sizes (64,128,256,512,512) and number of layers within a block (2,2,3,3,3) respectively. Since the number of filters differ across the blocks we shuffle the gating of the layers within each block in the reverse order. ResNet contains 3 blocks each with filter sizes (16,32,64) and number of layers within a block (36,36,36) respectively. The shuffling is done in a similar manner as VGG, i.e., the gating masks are reversed with each block.

### A.1 VGG-DLGN

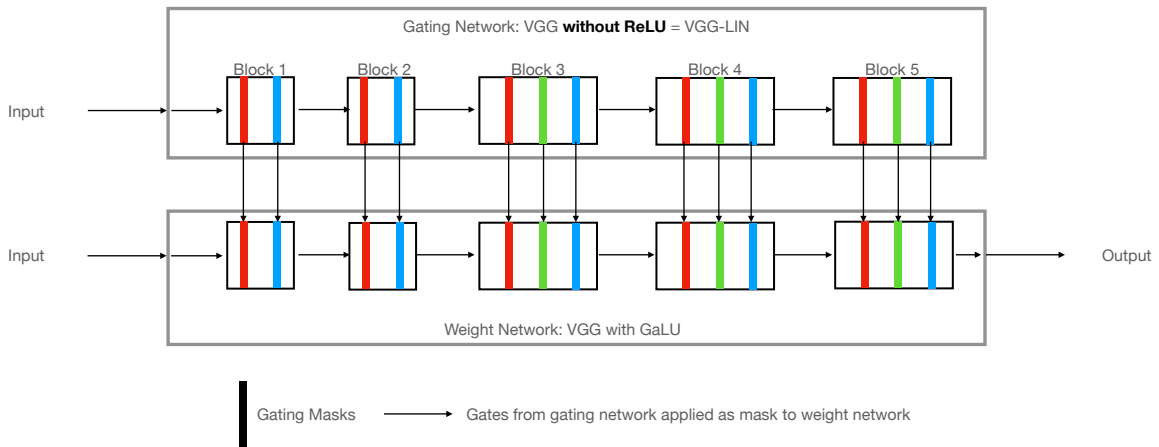


Figure 7: Shows VGG-DLGN

### A.2 VGG-DLGN-SHALLOW

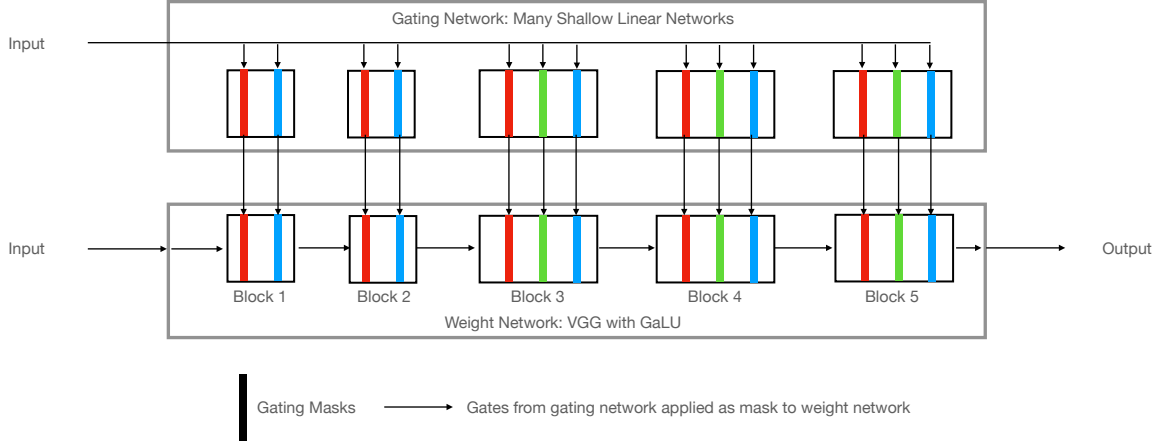


Figure 8: Shows VGG-DLGN-SHALLOW.

## B DGN Results without pre-training of the gating network

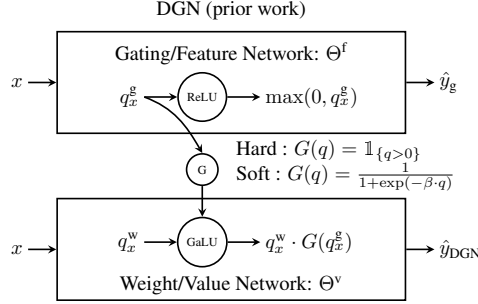
Architecture	Dataset	DNN	WITHOUT SHUFFLING		WITH SHUFFLING	
			DGN	DGN-ALLONES	DGN	DGN-ALLONES
FC4	MNIST	98.5 $\pm$ 0.1	98.2 $\pm$ 0.1	98.2 $\pm$ 0.1	98.1 $\pm$ 0.1	98.2 $\pm$ 0.1
CONV4	CIFAR-10	80.4 $\pm$ 0.3	77.2 $\pm$ 0.4	77.7 $\pm$ 0.3	77.3 $\pm$ 0.5	77.8 $\pm$ 0.6
VGG	CIFAR-10	93.6 $\pm$ 0.2	93.0 $\pm$ 0.1	93.0 $\pm$ 0.1	92.9 $\pm$ 0.1	92.9 $\pm$ 0.3
ResNet	CIFAR-10	94.0	93.3 $\pm$ 0.2	93.3 $\pm$ 0.1	92.9 $\pm$ 0.1	92.9 $\pm$ 0.2

Table 3: Table 2 showed the results when the gating network was pre-trained. This table shows the results when the gating network of the DGN is trained from scratch simultaneously alongside the weight network. The drop in 2 – 3% of the test accuracy when the gating network of teh DGNS are trained from scratch as opposed to a DGN with pre-trained gates has been documented by Lakshminarayanan and Singh [2020] and we observe that the same holds here as well. However, the most critical claim of this paper that providing a constant input as well as shuffling the gating masks does not **further** degrade the performance continues to hold even in the case when the gating network is trained from scratch is what is shown in this table. In other words, evidence provided by Table 2 to support our critical claims is not dependent on the fact that the gating network was pre-trained.

## C Other Related Works

**ReLU, Gating, Dual Linearity:** A spline theory based on max-affine linearity was proposed in [Balestriero et al., 2018, Balestriero and Baraniuk, 2018] to show that a DNN with ReLUs performs hierarchical, greedy template matching. In contrast, the dual view exploits the gating property to simplify the NTK into the NPK. Gated linearity was studied in [Fiat et al., 2019] for single layered networks, along with a non-gradient algorithm to tune the gates. The main novelty in our work in contrast to the above is that in DLGN the feature generation is linear. We refer to the gating property of the ReLU itself and has no connection to [Srivastava et al., 2015] where gating is a mechanism to regulate information flow. Also, the soft-gating in our work enables gradient flow via the gating network and is different from *Swish* [Ramachandran et al., 2018], which multiplies the pre-activation and sigmoid.

**Functional Role of Gating and Connection to Veness et al. [2019]:** There are both comparable and non-comparable aspects between our work and that of Gated Linear Networks (GLNs) of Veness et al. [2019]. The *non-comparable aspects* are (i) training: we use backpropagation to train DLGN vs Veness et al. [2019] propose a backpropagation free algorithm, (ii) learning in the gates: gates are learnable in our paper vs gates are fixed and random in Veness et al. [2019], and (iii) gating mechanism: more importantly Veness et al. [2019] presents only a fully connected GLN and convolutional/residual equivalents of GLNs are yet to be explored vs we have presented DLGN counterparts of state-of-the-art convolutional and residual models such as VGG-16 and ResNet-110. The comparable aspects is that the DGN/DLGN and the GLN have both separate gating and both models are essentially *data dependent linear networks*. It



is known that GLNs are good in continual learning tasks and given the similarity of the GLN and DLGN, an interesting future research direction would be to investigate the continual learning capabilities of the DLGN.

**Connection to Clark et al. [2021].** The connection between our paper and that of Clark et al. [2021] is through the dual view. To elaborate, Clark et al. [2021] deal with Vectorized Non-Negative Networks (VNN) whose special case (for the case when vector dimension equals 1) is a DNN with ReLUs with non-negative weights past first layer. As we understand, the key aspect of VNNs is the non-negativity of the weights past the first layer, and the non-negativity of the derivative of the activation function (which holds for Heaviside step function used in their paper), which enable a *global error vector broadcasting* (GEVB) rule, a non-backpropagation rule. We would like to point out that in VNN, the gating is not separate (however the authors mention in the context of vectorisation unfolding over time that gating can be made separate). We use dual view to disentangle DNNs with ReLUs, whereas, Clark et al. [2021] use the definitions of neural path activity and neural path value to show that the GEVB rule is sign aligned with the gradient of the VNNs. In particular, it is assumed that "for all training examples, each hidden unit has at least one active path with nonzero value connecting it to the output unit" (see page 17 of Clark et al. [2021]). Thus, the Clark et al. [2021] use the dual view to justify the GEVB rule, we use the dual view to in a much more fundamental way by disentangling the computations in a DNN with ReLUs and rearranging them in the form of DLGN to improve mathematical interpretability.

## D Deep Gated Network : Architecture and Training

The DGN is a setup to separate the gates from the weights. Consider a DNN with ReLUs with weights  $\Theta \in \mathbb{R}^{d_{net}}$ . The DGN *corresponding* to this DNN (left diagram in Figure 2) has two networks of *identical architecture* (to the DNN) namely the ‘gating network’ and the ‘weight network’ with distinct weights  $\Theta^f \in \mathbb{R}^{d_{net}}$  and  $\Theta^v \in \mathbb{R}^{d_{net}}$ . The ‘gating network’ has ReLUs which turn ‘on/off’ based on their pre-activation signals, and the ‘weight network’ has gated linear units (GaLUs) [Fiat et al., 2019, Lakshminarayanan and Singh, 2020], which multiply their respective pre-activation inputs by the external gating signals provided by the ‘gating network’. Since both the networks have identical architecture, the ReLUs and GaLUs in the respective networks have a one-to-one correspondence. Gating network realises  $\phi_{\Theta^f}(x)$  by turning ‘on/off’ the corresponding GaLUs in the weight network. The weight network realises  $v_{\Theta^v}$  and computes the output  $\hat{y}_{DGN}(x) = \langle \phi_{\Theta^f}(x), v_{\Theta^v} \rangle$ . The gating network is also called as the feature network since it realises the neural path features, and the weight network is also called as the value network since it realises the neural path value.

### D.1 DGN Training

The following two modes of training have been used in the paper namely **pretrained gates (PG)** and **standalone training (ST)**:

*Pretrained Gates (PG):* The gating network is pre-trained using  $\hat{y}_f$  as the output, and then the weights network is frozen, and the weights network is trained with  $\hat{y}_{DGN}$  as the output. Hard gating  $G(q) = \mathbb{1}_{\{q>0\}}$  is used.

*Standalone Training (ST):* Both gating and weight network are initialised at random and trained together with  $\hat{y}_{DGN}$  as the output. Here, soft gating  $G(q) = \frac{1}{1 + \exp(-\beta \cdot q)}$  is used to allow gradient flow through gating network. We tried several values of  $\beta$  in the range from 1 to 100, and found the range 4 to 10 to be suitable. We have chosen  $\beta = 10$  throughout the experiments.

### D.2 DLGN Training

In all the experiments the DLGN is trained in the **standalone training** mode.

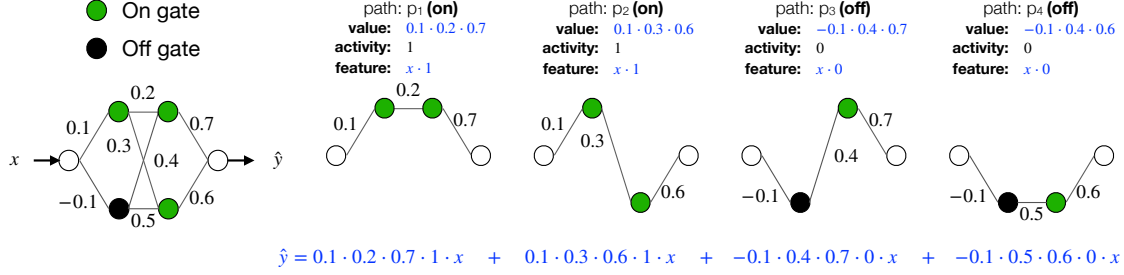


Figure 9: Illustration of dual view in a toy network with 2 layers, 2 gates per layer and 4 paths. Paths  $p_1$  and  $p_2$  are ‘on’ and paths  $p_3$  and  $p_4$  are ‘off’. The value, activity and feature of the individual paths are shown.  $\hat{y}$  is the summation of the individual path contributions.

## E Fully Connected

Here, we present the formal definition for the neural path features and neural path values for the fully connected case in Definition E.1. The layer-by-layer way of expressing the computation in a DNN of width ‘ $w$ ’ and depth ‘ $d$ ’ is given below.

Input Layer	:	$z_{x,\Theta}(\cdot, 0)$	=	$x$
Pre-Activation	:	$q_{x,\Theta}(i_{\text{out}}, l)$	=	$\sum_{i_{\text{in}}} \Theta(i_{\text{in}}, i_{\text{out}}, l) \cdot z_{x,\Theta}(i_{\text{in}}, l - 1)$
Gating	:	$G_{x,\Theta}(i_{\text{out}}, l)$	=	$\mathbf{1}_{\{q_{x,\Theta}(i_{\text{out}}, l) > 0\}}$
Hidden Layer Output	:	$z_{x,\Theta}(i_{\text{out}}, l)$	=	$q_{x,\Theta}(i_{\text{out}}, l) \cdot G_{x,\Theta}(i_{\text{out}}, l)$
Final Output	:	$\hat{y}_{\Theta}(x)$	=	$\sum_{i_{\text{in}}} \Theta(i_{\text{in}}, i_{\text{out}}, d) \cdot z_{x,\Theta}(i_{\text{in}}, d - 1)$

Table 4: Information flow in a FC-DNN with ReLU. Here, ‘ $q$ ’s are pre-activation inputs, ‘ $z$ ’s are output of the hidden layers, ‘ $G$ ’s are the gating values.  $l \in [d - 1]$  is the index of the layer,  $i_{\text{out}}$  and  $i_{\text{in}}$  are indices of nodes in the current and previous layer respectively.

**Notation** Index maps identify the nodes through which a path  $p$  passes. The ranges of index maps  $\mathcal{I}_l^f, \mathcal{I}_l, l \in [d - 1]$  are  $[d_{\text{in}}]$  and  $[w]$  respectively.  $\mathcal{I}_d(p) = 1, \forall p \in [P^{\text{fc}}]$ .

**Definition E.1.** Let  $x \in \mathbb{R}^{d_{\text{in}}}$  be the input to the DNN. For this input,

- (i)  $A_{\Theta}(x, p) \triangleq \prod_{l=1}^{d-1} G_{x,\Theta}(\mathcal{I}_l(p), l)$  is the activity of a path.
- (ii)  $\phi_{\Theta}(x) \triangleq \left( x(\mathcal{I}_0^f(p)) A_{\Theta}(x, p), p \in [P^{\text{fc}}] \right) \in \mathbb{R}^{P^{\text{fc}}}$  is the neural path feature (NPF).
- (iii)  $v_{\Theta} \triangleq \left( \prod_{l=1}^d \Theta(\mathcal{I}_{l-1}(p), \mathcal{I}_l(p), l), p \in [P^{\text{fc}}] \right) \in \mathbb{R}^{P^{\text{fc}}}$  is the neural path value (NPV).

## F Convolution With Global Average Pooling

In this section, we define NPFs and NPV in the presence of convolution with pooling. This requires three key steps (i) treating pooling layers like gates/masks (see Definition F.2) (ii) bundling together the paths that share the same path value (due to weight sharing in convolutions, see Definition F.3), and (iii) re-defining the NPF and NPV for bundles (see Definition F.4). Weight sharing due to convolutions and pooling makes the NPK rotationally invariant Lemma F.1. We begin by describing the architecture.

**Architecture:** We consider (for sake of brevity) a 1-dimensional<sup>2</sup> convolutional neural network with circular convolutions, with  $d_{\text{cv}}$  convolutional layers ( $l = 1, \dots, d_{\text{cv}}$ ), followed by a *global-average-pooling* layer ( $l = d_{\text{cv}} + 1$ ) and  $d_{\text{fc}}$  ( $l = d_{\text{cv}} + 2, \dots, d_{\text{cv}} + d_{\text{fc}} + 1$ ) fully connected layers. The convolutional window size is  $w_{\text{cv}} < d_{\text{in}}$ , the number of filters per convolutional layer as well as the width of the FC is  $w$ .

**Indexing:** Here  $i_{\text{in}}/i_{\text{out}}$  are the indices (taking values in  $[w]$ ) of the input/output filters.  $i_{\text{cv}}$  denotes the indices of the convolutional window taking values in  $[w_{\text{cv}}]$ .  $i_{\text{fout}}$  denotes the indices (taking values in  $[d_{\text{in}}]$ , the dimension of input features) of individual nodes in a given output filter. The weights of layers  $l \in [d_{\text{cv}}]$  are denoted by  $\Theta(i_{\text{cv}}, i_{\text{in}}, i_{\text{out}}, l)$  and

<sup>2</sup>The results follow in a direct manner to any form of circular convolutions.

for layers  $l \in [d_{fc}] + d_{cv}$  are denoted by  $\Theta(i_{in}, i_{out}, l)$ . The pre-activations, gating and hidden unit outputs are denoted by  $q_{x,\Theta}(i_{fout}, i_{out}, l)$ ,  $G_{x,\Theta}(i_{fout}, i_{out}, l)$ , and  $z_{x,\Theta}(i_{fout}, i_{out}, l)$  for layers  $l = 1, \dots, d_{cv}$ .

**Definition F.1** (Circular Convolution). For  $x \in \mathbb{R}^{d_{in}}$ ,  $i \in [d_{in}]$  and  $r \in \{0, \dots, d_{in} - 1\}$ , define :

- (i)  $i \oplus r = i + r$ , for  $i + r \leq d_{in}$  and  $i \oplus r = i + r - d_{in}$ , for  $i + r > d_{in}$ .
- (ii)  $rot(x, r)(i) = x(i \oplus r)$ ,  $i \in [d_{in}]$ .
- (iii)  $q_{x,\Theta}(i_{fout}, i_{out}, l) = \sum_{i_{cv}, i_{in}} \Theta(i_{cv}, i_{in}, i_{out}, l) \cdot z_{x,\Theta}(i_{fout} \oplus (i_{cv} - 1), i_{in}, l - 1)$ .

**Definition F.2** (Pooling). Let  $G_{x,\Theta}^{pool}(i_{fout}, i_{out}, d_{cv} + 1)$  denote the pooling mask, then we have

$$z_{x,\Theta}(i_{out}, d_{cv} + 1) = \sum_{i_{fout}} z_{x,\Theta}(i_{fout}, i_{out}, d_{cv}) \cdot G_{x,\Theta}^{pool}(i_{fout}, i_{out}, d_{cv} + 1),$$

where in the case of global-average-pooling  $G_{x,\Theta}^{pool}(i_{fout}, i_{out}, d_{cv} + 1) = \frac{1}{d_{in}}, \forall i_{out} \in [w], i_{fout} \in [d_{in}]$ .

Input Layer	:	$z_{x,\Theta}(\cdot, 1, 0)$	=	$x$
<b>Convolutional Layers, <math>l \in [d_{cv}]</math></b>				
Pre-Activation	:	$q_{x,\Theta}(i_{fout}, i_{out}, l)$	=	$\sum_{i_{cv}, i_{in}} \Theta(i_{cv}, i_{in}, i_{out}, l) \cdot z_{x,\Theta}(i_{fout} \oplus (i_{cv} - 1), i_{in}, l - 1)$
Gating Values	:	$G_{x,\Theta}(i_{fout}, i_{out}, l)$	=	$\mathbf{1}_{\{q_{x,\Theta}(i_{fout}, i_{out}, l) > 0\}}$
Hidden Unit Output	:	$z_{x,\Theta}(i_{fout}, i_{out}, l)$	=	$q_{x,\Theta}(i_{fout}, i_{out}, l) \cdot G_{x,\Theta}(i_{fout}, i_{out}, l)$
<b>GAP Layer, <math>l = d_{cv} + 1</math></b>				
Hidden Unit Output	:	$z_{x,\Theta}(i_{out}, d_{cv} + 1)$	=	$\sum_{i_{fout}} z_{x,\Theta}(i_{fout}, i_{out}, d_{cv}) \cdot G_{x,\Theta}^{pool}(i_{fout}, i_{out}, d_{cv} + 1)$
<b>Fully Connected Layers, <math>l \in [d_{fc}] + (d_{cv} + 1)</math></b>				
Pre-Activation	:	$q_{x,\Theta}(i_{out}, l)$	=	$\sum_{i_{in}} \Theta(i_{in}, i_{out}, l) \cdot z_{x,\Theta}(i_{in}, l - 1)$
Gating Values	:	$G_{x,\Theta}(i_{out}, l)$	=	$\mathbf{1}_{\{q_{x,\Theta}(i_{out}, l) > 0\}}$
Hidden Unit Output	:	$z_{x,\Theta}(i_{out}, l)$	=	$q_{x,\Theta}(i_{out}, l) \cdot G_{x,\Theta}(i_{out}, l)$
Final Output	:	$\hat{y}_{\Theta}(x)$	=	$\sum_{i_{in}} \Theta(i_{in}, i_{out}, d) \cdot z_{x,\Theta}(i_{in}, d - 1)$

Table 5: Shows the information flow in the convolutional architecture described at the beginning of Appendix F.

## F.1 Neural Path Features, Neural Path Value

**Proposition F.1.** The total number of paths in a CNN is given by  $P^{cnn} = d_{in}(w_{cv}w)^{d_{cv}}w^{(d_{fc}-1)}$ .

**Notation**[Index Maps] The ranges of index maps  $\mathcal{I}_l^f, \mathcal{I}_l^{cv}, \mathcal{I}_l$  are  $[d_{in}]$ ,  $[w_{cv}]$  and  $[w]$  respectively.

**Definition F.3** (Bundle Paths of Sharing Weights). Let  $\hat{P}^{cnn} = \frac{P^{cnn}}{d_{in}}$ , and  $\{B_1, \dots, B_{\hat{P}^{cnn}}\}$  be a collection of sets such that  $\forall i, j \in [\hat{P}^{cnn}], i \neq j$  we have  $B_i \cap B_j = \emptyset$  and  $\cup_{i=1}^{\hat{P}^{cnn}} B_i = [P^{cnn}]$ . Further, if paths  $p, p' \in B_i$ , then  $\mathcal{I}_l^{cv}(p) = \mathcal{I}_l^{cv}(p'), \forall l = 1, \dots, d_{cv}$  and  $\mathcal{I}_l(p) = \mathcal{I}_l(p'), \forall l = 0, \dots, d_{cv}$ .

**Proposition F.2.** There are exactly  $d_{in}$  paths in a bundle.

**Definition F.4.** Let  $x \in \mathbb{R}^{d_{in}}$  be the input to the CNN. For this input,

$$\begin{aligned} A_{\Theta}(x, p) &\triangleq \left( \prod_{l=1}^{d_{cv}+1} G_{x,\Theta}(\mathcal{I}_l^f(p), \mathcal{I}_l(p), l) \right) \cdot \left( \prod_{l=d_{cv}+2}^{d_{cv}+d_{fc}+1} G_{x,\Theta}(\mathcal{I}_l(p), l) \right) \\ \phi_{x,\Theta}(\hat{p}) &\triangleq \sum_{p \in B_{\hat{p}}} x(\mathcal{I}_0^f(p)) A_{\Theta}(x, p) \\ v_{\Theta}(B_{\hat{p}}) &\triangleq \left( \prod_{l=1}^{d_{cv}} \Theta(\mathcal{I}_l^{cv}(p), \mathcal{I}_{l-1}(p), \mathcal{I}_l(p), l) \right) \cdot \left( \prod_{l=d_{cv}+2}^{d_{cv}+d_{fc}+1} \Theta(\mathcal{I}_{l-1}(p), \mathcal{I}_l(p), l) \right) \end{aligned}$$

NPF	$\phi_{x,\Theta} \triangleq (\phi_{x,\Theta}(B_{\hat{p}}), \hat{p} \in [\hat{P}^{cnn}]) \in \mathbb{R}^{\hat{P}^{cnn}}$
NPV	$v_{\Theta} \triangleq (v_{\Theta}(B_{\hat{p}}), \hat{p} \in [\hat{P}^{cnn}]) \in \mathbb{R}^{\hat{P}^{cnn}}$

**Assumption F.1.**  $\Theta_0^v \stackrel{i.i.d}{\sim} \text{Bernoulli}(\frac{1}{2})$  over  $\{-\sigma, +\sigma\}$  and statistically independent of  $\Theta_0^f$ .



## F.2 Rotational Invariant Kernel

**Lemma F.1.**

$$\begin{aligned} \text{NPK}_{\Theta}^{\text{CONV}}(x, x') &= \sum_{r=0}^{d_{\text{in}}-1} \langle x, \text{rot}(x', r) \rangle \text{overlap}_{\Theta}(\cdot, x, \text{rot}(x', r)) \\ &= \sum_{r=0}^{d_{\text{in}}-1} \langle \text{rot}(x, r), x' \rangle \text{overlap}_{\Theta}(\cdot, \text{rot}(x, r), x') \end{aligned}$$

*Proof.* For the CNN architecture considered in this paper, each bundle has exactly  $d_{\text{in}}$  number of paths, each one corresponding to a distinct input node. For a bundle  $b_{\hat{p}}$ , let  $b_{\hat{p}}(i)$ ,  $i \in [d_{\text{in}}]$  denote the path starting from input node  $i$ .

$$\begin{aligned} & \sum_{\hat{p} \in [\hat{P}]} \left( \sum_{i, i' \in [d_{\text{in}}]} x(i)x'(i') A_{\Theta}(x, b_{\hat{p}}(i)) A_{\Theta}(x', b_{\hat{p}}(i')) \right) \\ &= \sum_{\hat{p} \in [\hat{P}]} \left( \sum_{i \in [d_{\text{in}}], i' = i \oplus r, r \in \{0, \dots, d_{\text{in}}-1\}} x(i)x'(i \oplus r) A_{\Theta}(x, b_{\hat{p}}(i)) A_{\Theta}(x', b_{\hat{p}}(i \oplus r)) \right) \\ &= \sum_{\hat{p} \in [\hat{P}]} \left( \sum_{i \in [d_{\text{in}}], r \in \{0, \dots, d_{\text{in}}-1\}} x(i) \text{rot}(x', r)(i) A_{\Theta}(x, b_{\hat{p}}(i)) A_{\Theta}(\text{rot}(x', r), b_{\hat{p}}(i)) \right) \\ &= \sum_{r=0}^{d_{\text{in}}-1} \left( \sum_{i \in [d_{\text{in}}]} x(i) \text{rot}(x', r)(i) \sum_{\hat{p} \in [\hat{P}]} A_{\Theta}(x, b_{\hat{p}}(i)) A_{\Theta}(\text{rot}(x', r), b_{\hat{p}}(i)) \right) \\ &= \sum_{r=0}^{d_{\text{in}}-1} \left( \sum_{i \in [d_{\text{in}}]} x(i) \text{rot}(x', r)(i) \text{overlap}_{\Theta}(i, x, \text{rot}(x', r)) \right) \\ &= \sum_{r=0}^{d_{\text{in}}-1} \langle x, \text{rot}(x', r) \rangle \text{overlap}_{\Theta}(\cdot, x, \text{rot}(x', r)) \end{aligned}$$

□

**Theorem F.1.** Let  $\sigma_{\text{cv}} = \frac{c_{\text{scale}}}{\sqrt{w}w_{\text{cv}}}$  for the convolutional layers and  $\sigma_{\text{fc}} = \frac{c_{\text{scale}}}{\sqrt{w}}$  for FC layers. Under Assumption F.1, as  $w \rightarrow \infty$ , with  $\beta_{\text{cv}} = \left( d_{\text{cv}} \sigma_{\text{cv}}^{2(d_{\text{cv}}-1)} \sigma_{\text{fc}}^{2d_{\text{fc}}} + d_{\text{fc}} \sigma_{\text{cv}}^{2d_{\text{cv}}} \sigma_{\text{fc}}^{2(d_{\text{fc}}-1)} \right)$  we have:

$$\text{NTK}_{\Theta_0^{\text{DGN}}}^{\text{CONV}} \rightarrow \frac{\beta_{\text{cv}}}{d_{\text{in}}^2} \cdot \text{NPK}_{\Theta_0}^{\text{CONV}}$$

*Proof.* Follows from Theorem 5.1 in [1].

□

## G Residual Networks with Skip connections

As a consequence of the skip connections, within the ResNet architecture there are  $2^b$  sub-FC networks (see ??). The total number of paths  $P^{\text{res}}$  in the ResNet is equal to the summation of the paths in these  $2^b$  sub-FC networks (see Proposition G.1). Now, The neural path features and the neural path value are  $P^{\text{res}}$  dimensional quantities, obtained as the concatenation of the NPFs and NPV of the  $2^b$  sub-FC networks.

**Proposition G.1.** The total number of paths in the ResNet is  $P^{\text{res}} = d_{\text{in}} \cdot \sum_{i=0}^b \binom{b}{i} w^{(i+2)d_{\text{blk}}-1}$ .

**Lemma G.1** (Sum of Product Kernel). Let  $\text{NPK}_{\Theta}^{\text{RES}}$  be the NPK of the ResNet, and  $\text{NPK}_{\Theta}^{\mathcal{J}}$  be the NPK of the sub-FCNs within the ResNet obtained by ignoring those skip connections in the set  $\mathcal{J}$ . Then,

$$\text{NPK}_{\Theta}^{\text{RES}} = \sum_{\mathcal{J} \in 2^{[b]}} \text{NPK}_{\Theta}^{\mathcal{J}}$$

*Proof.* Proof is complete by noting that the NPF of the ResNet is a concatenation of the NPFs of the  $2^b$  distinct sub-FC-DNNs within the ResNet architecture.  $\square$

**Theorem G.1.** Let  $\sigma = \frac{c_{scale}}{\sqrt{w}}$ . Under Assumption F.1, as  $w \rightarrow \infty$ , for  $\beta_{res}^{\mathcal{J}} = (|\mathcal{J}| + 2) \cdot d_{blk} \cdot \sigma^{2((|\mathcal{J}|+2)d_{blk}-1)}$ ,

$$NTK_{\Theta_0^{DGN}}^{RES} \rightarrow \sum_{\mathcal{J} \in 2^{[b]}} \beta_{res}^{\mathcal{J}} NPK_{\Theta_0^f}^{\mathcal{J}}$$

*Proof.* Follows from Theorem 5.1 in [1].  $\square$

## H Numerical Experiments: Setup Details

We now list the details related to the numerical experiments which have been left out in the main body of the paper.

- Computational Resource. The numerical experiments were run in Nvidia-RTX 2080 TI GPUs and Tesla V100 GPUs.
- All the models other than VGG and ResNet (and their variants) we used Adam [Kingma and Ba, 2014] with learning rate of  $3 \times 10^{-4}$ , and batch size of 32.
- All the VGG-16, Resnet-110 (and their DGN/DLGN) models we used *SGD* optimiser with momentum 0.9 and the following learning rate schedule (as suggested in Mikler [2019]) : for iterations  $[0, 400)$  learning rate was 0.01, for iterations  $[400, 32000)$  the learning rate was 0.1, for iterations  $[32000, 48000)$  the learning rate was 0.01, for iterations  $[48000, 64000)$  the learning rate was 0.001. The batch size was 128. The models were trained till 32 epochs.